

**Copyright
by
Ryan Patrick Hannigan
2023**

The Dissertation Committee for Ryan Patrick Hannigan certifies that
this is the approved version of the following dissertation:

Stranger Things at the LHC

Committee:

Christina Markert, Supervisor

Peter Onyisi

Richard Hazeltine

Chandrajit Bajaj

Stranger Things at the LHC

by

Ryan Patrick Hannigan, B.S.

Dissertation

Presented to the Faculty of the Graduate School of
The University of Texas at Austin
in Partial Fulfillment
of the Requirements
for the degree of
Doctor of Philosophy

The University of Texas at Austin
May, 2023

To Jaynee, who unquestionably is the reason why this document exists.

Contents

List of Figures	vi
List of Tables	viii
Chapter One: Introduction	1
1.1 What is fundamental?	2
1.2 The Standard Model	8
1.3 Quantum chromodynamics	10
1.4 Heavy ion collisions	19
1.5 Theoretical models	23
Bibliography	27

List of Figures

1.1	Dimitri Mendeleev’s periodic table of elements from the late 1800s, taken from [4]. The elements are grouped by similar chemical properties, and the gaps in the table are where Mendeleev predicted that new elements would be discovered.	2
1.2	The “Eightfold Way” diagrams of the $J = 1/2$ mesons (left) and $J = 3/2$ baryons (right) plotted against strangeness and electric charge. Understanding the underlying symmetry group that gives rise to such patterns ¹ ultimately led to the development of the quark model. While the original patterns were found using isotopic spin and hypercharge, it is trivial to convert between the two using the Gell-Mann-Nishijima formula [19], [20].	4
1.3	The energy distribution of electrons scattered off of protons at an initial electron energy of 10 GeV and a scattering angle of 6 degrees. The large spike on the left side of the distribution corresponds to the elastic scattering of the electron off the proton, and the “bumps” correspond to the inelastic scattering of the electron off the proton. The “background” underneath the bumps and the apparent continuum of events at even lower values of the scattered electron energy correspond to a mess of unknown particles being produced. The behavior of this continuum with respect to the scattering angle and the scattered electron energy ultimately led to the conclusion that the proton was not fundamental.	6
1.4	A schematic of the field lines between two electrically charged particles (left) and two quarks (right). The field lines between the quarks are pulled together due to the self-interaction of the gluons, whereas the electric field lines are not.	14
1.5	The value of the strong coupling constant α_s as a function of momentum transfer Q , which represents the energy scale of the interaction.	15
1.6	A diagram depicting the formation of a jet within the Lund model from an initial hard scattering of partons, adapted from [41]. The vertices represent perturbative QCD processes, the shaded regions represent string fragmentation/hadronization, and the outgoing arrows represent the resulting hadrons (which may decay further).	16

1.7	A phase diagram of the QGP, taken from QGPPhaseDiagram . The axes are temperature and baryon density, and the orange band represents the phase transition from normal hadronic matter to the QGP.	17
1.8	A schematic of the evolution of the universe, taken from QGPUniverse . The QGP phase of the universe on this diagram lies roughly between 10^{-10} and 10^{-5} seconds after the Big Bang.	18
1.9	A schematic of the formation and evolution of the QGP in a heavy ion collision. The QGP is formed in the overlap region of the two colliding nuclei, and then expands and cools very quickly.	20
1.10	A schematic of a heavy ion collision with impact parameter b , taken from ??.	21
1.11	The distribution of Pb–Pb collision events as a function of event activity in the ALICE VZERO detector, taken from ALICECentrality	23
1.12	A schematic of the parton ladder in the EPOS LHC model.	25

List of Tables

1.1 The fermions of the Standard Model for each generation and their corresponding multiplets. The Standard Model does not allow for fermions to leave their respective multiplets.	10
---	----

Chapter One: Introduction

This initial section of this chapter will mostly serve as a historical overview of the field of particle physics, leading to the development of the **Standard Model**—the theory that describes all of the fundamental¹ particles and the way in which they interact with each other. An emphasis will be made on the discovery of quarks, as the research presented in this thesis is centered around these particles. This section will contain little-to-no mathematics, as historical lessons generally do not.

The second section will more thoroughly introduce the Standard Model, and how it was developed from a theoretical perspective. Words like “fundamental representation” and “gauge symmetry” will be thrown around, but the goal is to provide a high-level mathematical overview of the theory and how it was developed without getting bogged down in the details.

As this thesis is focused nearly entirely on the strong nuclear force, the remaining sections of the chapter will delve into the details of Quantum ChromoDynamics (QCD), which is the component of the Standard Model which describes the interactions between **quarks** and **gluons**—the constituent particles of the more familiar protons and neutrons. Unfortunately, QCD is enormously complicated and the full theory is not yet fully understood. While this may be disheartening for theorists, it is a boon for experimentalists as it provides a wealth of opportunities to probe the theory in regimes where it is both understood and not understood.

To that end, the remainder of the chapter will focus on the ways in which QCD can be investigated using heavy-ion collisions, with an emphasis on the **Quark-Gluon Plasma** (QGP)—a novel state of nuclear matter that QCD predicts should exist at the extreme temperatures and densities that are achieved in these collisions. The experimental signatures of QGP formation will also be discussed, with a particular focus on **strangeness enhancement**—the phenomenon where the production of strange quarks is enhanced in heavy-ion collisions relative to proton-proton collisions.

¹As of the year 2023, but reading this chapter will hopefully illustrate why this may be subject to change in the (likely very distant) future.

1.1 What is fundamental?

The answer to the question “What are the fundamental building blocks of our universe?” has changed drastically over the course of human history. The idea that all matter is composed of smaller, uncuttable pieces has been around since 5th century BCE when Greek philosophers Democritus and Leucippus first introduced the concept of an atom [1]. While this idea was mostly motivated by philosophical reasoning, it was later adopted by the English scientist John Dalton in the 19th century to explain the results of his chemical experiments, where he found that chemical elements always combined with each other by discrete units of mass [2]. As scientists discovered more and more of these elements, the number of “fundamental” building blocks grew as well. By the late 1800s, over 70 unique chemical elements had been discovered, though they would often be grouped together due to similar chemical properties using what chemist Dimitri Mendeleev dubbed the *periodic table of elements* [3]. An example of the periodic table from the time of Mendeleev can be seen in Figure 1.1. While this grouping was useful for chemists, it also served as a hint to physicists that perhaps these elements were not actually fundamental, but rather composed of even smaller pieces.

		Ti = 50	Zr = 90	? = 180
		V = 51	Nb = 94	Ta = 182
		Cr = 52	Mo = 96	W = 186
		Mn = 55	Rh = 104,4	Pt = 197,4
		Fe = 56	Ru = 104,4	Ir = 198
		Ni = 59	Pd = 106,6	Os = 199
H = 1		Cu = 63,4	Ag = 108	Hg = 200
	Be = 9,4	Mg = 24	Zn = 65,2	Cd = 112
	B = 11	Al = 27,4	? = 68	Ur = 116
	C = 12	Si = 28	? = 70	Sn = 118
	N = 14	P = 31	As = 75	Sb = 122
	O = 16	S = 32	Se = 79,4	Te = 128?
	F = 19	Cl = 35,5	Br = 80	J = 127
Li = 7	Na = 23	K = 39	Rb = 85,4	Cs = 133
		Ca = 40	Sr = 87,6	Tl = 204
		? = 45	Ce = 92	Ba = 137
		?Er = 56	La = 94	Pb = 207
		?Yt = 60	Di = 95	
		?In = 75,6	Th = 118?	

Figure 1.1: Dimitri Mendeleev’s periodic table of elements from the late 1800s, taken from [4]. The elements are grouped by similar chemical properties, and the gaps in the table are where Mendeleev predicted that new elements would be discovered.

Things changed quite a bit around the turn of the 20th century, with scientists like Rutherford and Chadwick determining that the supposedly indivisible atom was

composed of even smaller sub-atomic particles, eventually named electrons, protons and neutrons [5]–[7]. Thus the number of fundamental blocks of matter had decreased substantially from nearly 100 to just three, but only very briefly. Only months after the discovery of the neutron, the fundamental anti-particle of the electron—known as the positron—was discovered in 1932 by Carl Anderson [8]. In the next two decades, the number of known fundamental particles would skyrocket. In 1947, the muon was discovered [9], followed by the discovery of a laundry list of particles [10]–[12] that participate in the same interaction that holds oppositely charged protons together in the nucleus of an atom—the so-called **strong nuclear force**. These “fundamental” particles were collectively called **hadrons**, which were further separated into lighter and heavier categories dubbed **mesons** and **baryons**, respectively [13]. By the late 1960s, the number of known hadrons had grown to well over 100 [14], which is a far cry from the number of “fundamental” chemical elements that were known to exist in the 1800s.

In the same way that Mendeleev tried to group the elements by their similar chemical properties, physicists attempted to group the hadrons together based on their known sub-atomic properties at the time. The first successful attempt at such a grouping was the **Eightfold Way**, which was independently proposed by Murray Gell-Mann and Yuval Ne’eman in 1961 [15], [16]. This grouping was found by examining the following properties of the hadrons:

1. **Isotopic spin:** a quantum number introduced by Werner Heisenberg in 1932 to try to explain the apparent symmetries between the proton and neutron with respect to the strong nuclear force [17] (i.e. although the proton and neutron have different electric charges, the strong interaction does not seem to distinguish between the two)
2. **Strangeness:** another quantum number introduced by Gell-Mann and Nishijima in 1953 to explain why some hadrons decayed much more slowly than expected, but such particles appeared to be created in pairs [18]. In other words, the strong interaction responsible for the creation of these particles appeared to conserve strangeness, but the weak interaction responsible for the slower decay of these particles did not. This² quantity is of utmost importance to this thesis,

²Strangeness was introduced a few years before the very first quark model, but it now has the modern interpretation which is directly related to the number of strange and anti-strange quarks

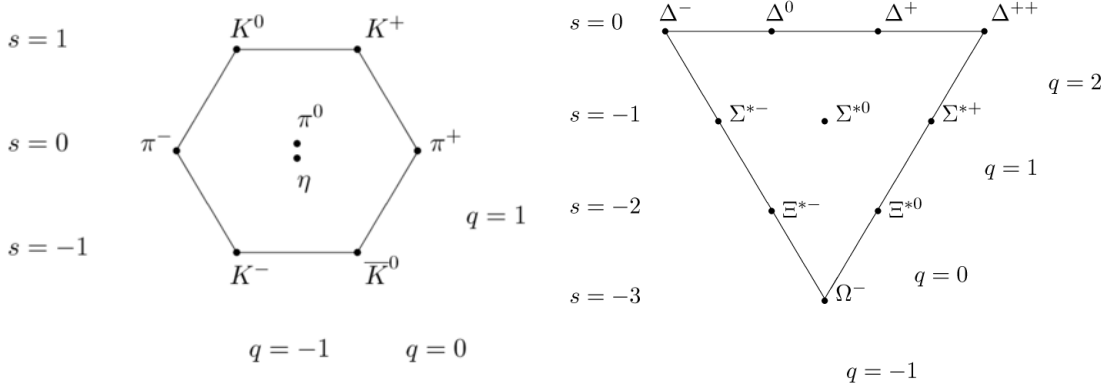


Figure 1.2: The “Eightfold Way” diagrams of the $J = 1/2$ mesons (left) and $J = 3/2$ baryons (right) plotted against strangeness and electric charge. Understanding the underlying symmetry group that gives rise to such patterns³ ultimately led to the development of the quark model. While the original patterns were found using isotopic spin and hypercharge, it is trivial to convert between the two using the Gell-Mann-Nishijima formula [19], [20].

and will be discussed in much greater detail in the coming sections.

Plotting the baryons and mesons in a two-dimensional space based on these two properties revealed striking patterns, as shown in Figure 1.2. Similar to Mendeleev, GellMann also left a blank space⁴ where he believed a new particle—the Ω^- —would be discovered. The patterns in these diagrams hinted at an underlying symmetry governing the strong nuclear force, and ultimately led to the invention of the very first quark model by Gell-Mann and Zweig in 1964 [21]. This model proposed that all of the hadrons were actually composed of even smaller particles, which Gell-Mann dubbed “quarks”. The quark model was able to explain the patterns seen in Figure 1.2 by introducing three different types of fermionic quarks—up, down and strange—along with their corresponding anti-quarks. Baryons would then be composed of three such quarks, whereas mesons would be composed of quark and anti-quark pairs. If the quark model were correct, the number of fundamental building blocks of matter would

within a hadron.

³Namely SU(3), but this is a history lesson. Also the path from SU(3) to patterns of this type is long and arduous, involving a thorough understanding of representation theory.

⁴The original paper on the Eightfold Way does not contain any of these diagrams, but there are discussions about the properties of particles that should exist if the theory were correct, but had not been observed [15].

again decrease from over 100 to just 14: electrons, muons, electron neutrinos, muon neutrinos, up quarks, down quarks, strange quarks, and all of their corresponding anti-particles.

Initially, many physicists believed that the quarks from this model were just a mathematical abstraction [22]. This possibility did not stop Sheldon Glashow and James Bjorken from extending the quark model in less than a year after its inception by introducing a fourth quark: the charm [23]. This new quark was primarily introduced to equalize the number of leptons (four at the time: electron, muon, and their respective neutrinos) with the number of quarks. The theory was mostly aesthetic [24] in that the charm quark was not explicitly required by any known mechanisms. It was only after the Glashow-Iliopoulos-Maiani (GIM) mechanism was introduced in 1970 [25] that the existence of the charm quark became “necessary”. This mechanism helped explain why neutral kaons decayed into two muons at a much lower rate than expected, but it required the existence of a quark with the same charge as the up quark but with a much larger mass.

On the experimental side of things, the notion that protons and neutrons were fundamental particles was also being challenged. The deep inelastic scattering experiments at the Standford Linear Accelerator Center (SLAC) performed by Kendall, Friedman and Taylor in 1968 [26]–[28] revealed unexpected⁵ behavior when probing the structure of the proton: it appeared to be composed of point-like particles. These experiments were performed by firing electrons at stationary protons and measuring the energy distributions of the scattered electrons at different scattering angles. An example such a distribution for electrons with initial energies of 10 GeV scattered at 6 degrees can be seen in Figure 1.3. The large spike on the left side of the distribution corresponds to the elastic scattering of the electron off the proton, which was well understood at the time [29]. The “bumps” observed at lower values of the scattered electron energy were also well understood [30], and they correspond to the “shallow” inelastic scattering of the electron off the proton, where the proton gets excited into a so-called *resonance* state (like the Δ baryon). However, the “background” underneath the bumps and the apparent continuum of events at even lower values of the scattered electron energy correspond to a mess of unknown particles being produced. This mess of particles appeared to grow with increasing scattering angle and de-

⁵Depending on who you asked at the time, both the three and four quark models were not universally accepted.

ing scattered electron energy, which ultimately led to the conclusion that the proton was composed of point-like particles that were being “knocked out” of the proton by the incoming electron [26], [31].

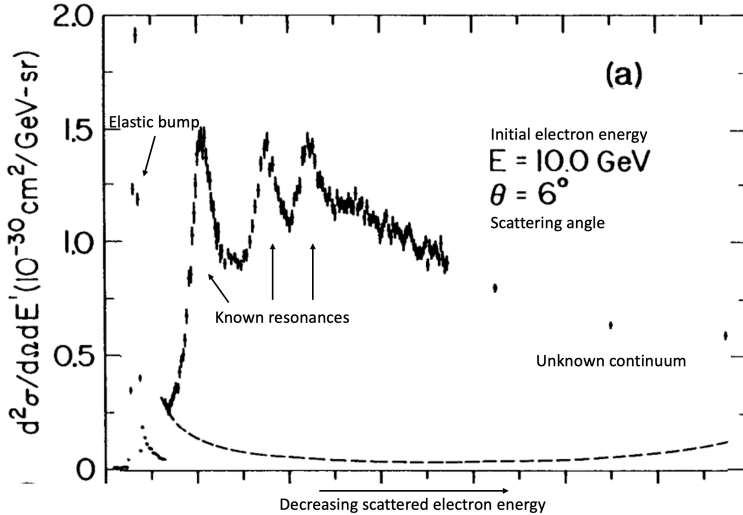


Figure 1.3: The energy distribution of electrons scattered off of protons at an initial electron energy of 10 GeV and a scattering angle of 6 degrees. The large spike on the left side of the distribution corresponds to the elastic scattering of the electron off the proton, and the “bumps” correspond to the inelastic scattering of the electron off the proton. The “background” underneath the bumps and the apparent continuum of events at even lower values of the scattered electron energy correspond to a mess of unknown particles being produced. The behavior of this continuum with respect to the scattering angle and the scattered electron energy ultimately led to the conclusion that the proton was not fundamental.

While many physicists were perfectly happy to interpret these point-like particles as the very same quarks from the aforementioned quark model(s), they received the much more noncommittal name **partons** after Richard Feynman’s parton model of hadrons [32]. The association of these partons with quarks was not universally accepted⁶ until the discovery of the J/ψ meson in 1974 [33]. In the meantime, the theoretical description of the strong nuclear force was closing in on its final form. The formulation of Quantum ChromoDynamics (QCD) in the early 1970s by Gell-Mann, Fritzsch, and Leutwyler [34] resolved many of the issues that were present in

⁶No acceptance of any model is a step function, but the discovery of J/ψ seems to be a turning point in literature.

the initial quark models⁷. QCD introduced the concept of color charge, which all of the quarks would carry. The mediating bosons of the strong interaction—known as **gluons**—were also introduced⁸.

While QCD gave a solid mathematical description of the strong interaction, it wasn't until the discovery of **asymptotic freedom** [35], [36] by Gross, Wilczek and Politzer in 1973 that the theory became experimentally testable. Asymptotic freedom is the notion that the strong interaction becomes weaker at higher energies, allowing for QCD calculations to be performed using perturbative techniques. This discovery allowed theorists to use QCD to make predictions of the results of very high energy particle collision experiments. The first QCD prediction to be experimentally verified came from the Positron-Electron Tandem Ring Accelerator (PETRA) in 1979 [37], which experimentally confirmed the existence of gluons [38]. With experimental verification of QCD, it became clear that the association of partons with quarks was indeed incorrect: they are both quarks *and* gluons.

While not of particular import to this thesis⁹, the theory of electroweak interactions was also being developed during the 1960s by Glashow, Weinberg and Salam [39], [40]. With this new theory came the prediction of four¹⁰ new bosons: the Higgs boson, the charged W^\pm bosons, and the neutral Z^0 boson. With the combined theories of the electroweak and strong interaction, the **Standard Model** of particle physics—which describes the now 61¹¹ fundamental particles and how they interact—was complete.

⁷For example, the wavefunction of the Δ^{++} baryon under the first quark model was not anti-symmetric, which is a requirement for fermions.

⁸And also carried color charge, but more details will be discussed in Section 1.3

⁹Though extremely interesting in its own right

¹⁰The Higgs mechanism (which predicts the existence of the Higgs boson) came before electroweak unification **HiggsPaper**, but it was a requirement for the theory.

¹¹There are many ways to count fundamental particles, but this particular number is obtained by: 6 leptons ($\times 2$ for anti-leptons), 6 quarks ($\times 3$ for each color, $\times 2$ for anti-quarks), 1 gluon ($\times 8$ for color), 1 photon, the W and Z bosons, and the Higgs boson. The more common number of seventeen **ParticleNumber** is a bit low, especially given that anti-particles have already been counted in the earlier parts of this section.

1.2 The Standard Model

The Standard Model of particle physics is a **quantum field theory** (QFT) that describes the interactions between all¹² of the fundamental particles. QFTs describe the dynamics of a quantum system in terms of fields, which are functions of space and time. The fields are the fundamental objects of QFT, and their excitations correspond to the particles that are observed in nature. The Standard Model fields can be broken down into three sectors, which will be discussed in the following sections.

1.2.1 The gauge sector

The gauge sector of the Standard Model corresponds to the spin-one bosons that mediate the strong and electroweak interactions. In a general sense, this sector corresponds to the mediating particles for three of the four fundamental forces: the strong nuclear force, the weak nuclear force, and the electromagnetic force. The fourth fundamental force—gravity—is not included in the Standard Model, as it is not yet understood from a quantum perspective **QuantumGravity**.

The symmetry group of the gauge sector is given by

$$\mathrm{SU}(3)_c \times [\mathrm{SU}(2)_L \times \mathrm{U}(1)_Y]. \quad (1.1)$$

$\mathrm{SU}(3)_c$ is the symmetry group of the strong interaction, which is described by the QFT known as Quantum ChromoDynamics (QCD). The subscript c stands for “color”, indicating that the gauge fields in QCD (gluons) only couple to colored objects. As QCD is the theory that mostly describes the research presented in this thesis, it will be discussed in much greater detail in Section 1.3. The symmetry group of the electroweak interaction is $\mathrm{SU}(2)_L \times \mathrm{U}(1)_Y$, where the subscript L stands for “left-handed” and the subscript Y stands for “weak hypercharge”. Again, these subscripts indicate the types of objects to which the corresponding gauge fields couple. For example, the gauge fields of $\mathrm{SU}(2)_L$ only couple to left-handed objects, and the gauge fields of $\mathrm{U}(1)_Y$ only couple to weakly hypercharged objects. Initially, there are four massless gauge fields in the theory¹³. After the spontaneous symmetry breaking of the Higgs mechanism **HiggsMechanism**, these fields mix to give rise to three

¹²Ignoring potential gravitons **Graviton** or dark matter candidates **DarkMatter1**, **DarkMatter2**

¹³Three corresponding to the generators of $\mathrm{SU}(2)$, one corresponding to the generator of $\mathrm{U}(1)$.

massive gauge fields and one massless gauge field. The three massive gauge fields correspond to the familiar W^\pm and Z^0 bosons, which are the mediating bosons of the weak interaction. The massless gauge field corresponds to the photon, which mediates the electromagnetic interaction.

1.2.2 The scalar sector

The scalar sector of the Standard Model is quite lonely, and only corresponds to one spin-zero field: the Higgs **PeterHiggs**. As mentioned in the previous section, the Higgs mechanism that corresponds to this field is responsible for the acquisition of mass by the W^\pm and Z^0 bosons. The Higgs field also couples to all of the fermions in the Standard Model, but the mass acquisition procedure is *slightly* different¹⁴. The associated Higgs boson was discovered by the A Toroidal LHC Apparatus (ATLAS) and Compact Muon Solenoid (CMS) collaborations in 2012 **HiggsDiscovery1**, **HiggsDiscovery2**, and was the last major piece of the Standard Model to be experimentally verified.

1.2.3 The fermionic sector

The fermionic sector contains all of the spin one-half particles (quarks and leptons) in the Standard Model. It is often convenient to group these particles into three generations, where each generation is identical except for the masses of the particles. It is even *more* convenient to group the fermions within each family into multiplets, where the members of the multiplet are related to each other by transformations within the gauge group of the Standard Model (Equation 1.1). In other words, the fermions within a particular multiplet can only be transformed to fermions within the same multiplet. A table of the fermions in the Standard Model and their corresponding multiplets can be seen in Table 1.2.3. The indices L and R correspond to the chirality of the fields, and the indices r , g and b represent to the color charge of the fields. The color charges are only non-zero for the quarks, making them a key component of quantum chromodynamics.

¹⁴It's still spontaneous symmetry breaking, but within the Yukawa part of the electroweak Lagrangian.

Table 1.1: The fermions of the Standard Model for each generation and their corresponding multiplets. The Standard Model does not allow for fermions to leave their respective multiplets.

Gen.	Left-handed quarks	Right-handed up quarks	Right-handed down quarks	Left- handed leptons	Right- handed leptons
1 st gen.	$\begin{pmatrix} u_L^r & u_L^g & u_L^b \\ d_L^r & d_L^g & d_L^b \end{pmatrix}$	$(u_R^r \ u_R^g \ u_R^b)$	$(d_R^r \ d_R^g \ d_R^b)$	$\begin{pmatrix} \nu_{eL} \\ e_L \end{pmatrix}$	(e_R)
2 nd gen.	$\begin{pmatrix} c_L^r & c_L^g & c_L^b \\ s_L^r & s_L^g & s_L^b \end{pmatrix}$	$(c_R^r \ c_R^g \ c_R^b)$	$(s_R^r \ s_R^g \ s_R^b)$	$\begin{pmatrix} \nu_{\mu L} \\ \mu_L \end{pmatrix}$	(μ_R)
3 rd gen.	$\begin{pmatrix} t_L^r & t_L^g & t_L^b \\ b_L^r & b_L^g & b_L^b \end{pmatrix}$	$(t_R^r \ t_R^g \ t_R^b)$	$(b_R^r \ b_R^g \ b_R^b)$	$\begin{pmatrix} \nu_{\tau L} \\ \tau_L \end{pmatrix}$	(τ_R)

1.3 Quantum chromodynamics

This section serves as a turning point for this thesis: while the discussions above have been *mostly* general, the novel research presented in this thesis is centered around the strong nuclear force. As such, the remainder of this chapter will delve into the details of this mysterious force, and how it can be studied using high-energy particle collisions.

1.3.1 The QCD Lagrangian

The dynamics of these fields and how they interact are completely encoded within the Lagrangian of the theory, which can be used to calculate experimental observables like cross sections and decay rates. The Lagrangian of the Standard Model is fairly long **StandardModelLength1**, **StandardModelLength2**, and often not particularly insightful when trying to study a specific aspect of the theory. As such, when studying QCD, it is often useful to throw away the electroweak gauge fields, leptons, and scalars to give only the QCD Lagrangian **QCDLagrangian**,

$$\begin{aligned} \mathcal{L}_{QCD} = & -\frac{1}{4}F_{\mu\nu}^A F^{A\mu\nu} + i\bar{q}\gamma^\mu \left(\partial_\mu + ig_s \frac{1}{2} \lambda^A \mathcal{A}_\mu^A \right) q \\ & - \bar{q}_R \mathcal{M} q_L - \bar{q}_L \mathcal{M}^\dagger q_R - \theta\omega, \end{aligned}$$

where all repeated indices are summed over.

The gluons are described by the vector gauge field \mathcal{A}_μ^A , with index A representing one of the eight color labels. These eight components belong to the color group

$SU_c(3)$, which is the gauge group of QCD. The corresponding coupling constant is g_s , and the field strength tensor $F_{\mu\nu}^A$ is given by

$$F_{\mu\nu}^A = \partial_\mu A_\nu^A - \partial_\nu A_\mu^A + g_s f^{ABC} A_\mu^B A_\nu^C, \quad (1.2)$$

where f^{ABC} are the structure constants **StructureConstants** of $SU_c(3)$. Note that while this field strength tensor shares the same letters as the electromagnetic field strength tensor $F_{\mu\nu}$, the additional term $g_s f^{ABC} A_\mu^B A_\nu^C$ in Equation 1.2 separates QCD and QED in a very fundamental way: the gluons are allowed to self-interact. This self-interaction is a direct result of the non-vanishing structure constants of $SU_c(3)$ ¹⁵, and causes a lot of headaches for theorists.

The quarks are represented by the field q , which is a bit misleading as the color, flavor and spin indices have been suppressed. In reality, the quark field q has:

- six flavor indices $\{u, d, s, c, b, t\}$,
- four spin indices $\{0, 1, 2, 3\}$, and
- three color indices $\{r, g, b\}$,

where all of these indices are being implicitly summed over in \mathcal{L}_{QCD} . Luckily all of the matrices $(A_\mu^A, \lambda^A, \mathcal{M}, \gamma^\mu)$ act on separate sets of indices¹⁶. For example, the γ^μ 's only operate on the spin indices, whereas both the gluon fields A_μ^A and Gell-Mann matrices **GellMannMatrix** λ^A operate on the color indices. These Gell-Mann matrices are the generators of $SU_c(3)$ and satisfy the commutation relation

$$[\lambda^A, \lambda^B] = 2i f^{ABC} \lambda^C. \quad (1.3)$$

The chiral quark fields q_L and q_R are defined as $\frac{1}{2}(1-\gamma_5)q$ and $\frac{1}{2}(1+\gamma_5)q$, respectively. The mass matrix \mathcal{M} operates on the flavor indices, and its form depends on the choice of basis for the quark fields **QCDHistory**. It is often convenient to choose a basis where the mass matrix is diagonal, which can be done by independent rotations of q_L and q_R in $SU(6)$. Doing so gives the more familiar term

$$-\bar{q}_R \mathcal{M} q_L - \bar{q}_L \mathcal{M}^\dagger q_R = - \sum_{f=1}^6 \bar{q}_f m_f q_f, \quad (1.4)$$

¹⁵Structure constants of Abelian gauge groups like $U(1)$ are trivially zero.

¹⁶Really the components of the field corresponding to those indices.

where m_f is the mass of the quark with flavor f , and q_f is the flavor component of the quark field. Note that this term completely violates the $SU(2) \times U(1)$ electroweak symmetry, indicating that the given \mathcal{L}_{QCD} is determined *after* the spontaneous symmetry breaking described in the previous section. These quark masses are also subject to renormalization **MassRenorm**, which results in the running of the quark mass with respect to the energy scale of the interaction¹⁷. More simply, the quark masses are inversely dependent on this energy scale: at large energies, the quark masses are small, and at low energies, the quark masses are large.

The final terms θ and ω correspond to the QCD vacuum angle and winding number density, respectively **VacuumAngle**, **WindingNumber**.

1.3.1.1 Brief aside: Why eight gluons?

The gluon field \mathcal{A}^A transforms under the adjoint representation of $SU(3)$, which is a representation of $SU(3)$ on the vector space of its Lie algebra $\mathfrak{su}(3)$. As $\mathfrak{su}(3)$ has eight basis elements (for instance, the Gell-Mann matrices λ^A from above), the adjoint representation of $SU(3)$ is eight-dimensional. Thus the gluon field has eight independent components, or there are eight gluons. In principle, QCD could have been built on top of a $U(3)$ gauge group, which would give rise to nine gluons (as the dimension of $U(n)$ is n^2). However, the singlet state in $U(3)$ must not be interacting: if it were, color neutral baryons would interact with each other via the strong interaction at a much longer range **SingletGluons**. Such interactions have not been observed **SingletGluons2**. As there is no physical difference between $U(3)$ with a non-interacting singlet and $SU(3)$, the simpler gauge group was chosen.

As an aside to the current aside, a lot of fun can be had with the adjoint representation of $SU(3)$. For example, the term $g_s f^{ABC} \mathcal{A}^B \mathcal{A}^C$ can be thought of as boring 3×3 matrix multiplication, but it can also be thought of as an inner product between two eight-dimensional row/column vectors. Unfortunately the fun breaks down at some point, as terms like $i\bar{q}\gamma^\mu (ig_s \frac{1}{2} \lambda^A \mathcal{A}_\mu^A) q$ can only be interpreted as \mathcal{A} transforming q under the fundamental representation of $SU(3)$ (i.e. 3×3 matrix acting on 3×1 vector). Furthermore, writing λ^A as an 8×8 matrix is not particularly enlightening—though

¹⁷They also depend on the *choice* of renormalization scheme, with the most commonly implemented one being minimal subtraction or MS **MSScheme**.

it can be done. For example, λ^1 in the adjoint representation is given by

$$\lambda^{1,\text{adjoint}} = \begin{pmatrix} 0 & 0 & 0 & 0 & 0 & 0 & 0 & 0 \\ 0 & 0 & -2i & 0 & 0 & 0 & 0 & 0 \\ 0 & 2i & 0 & 0 & 0 & 0 & 0 & 0 \\ 0 & 0 & 0 & 0 & 0 & 0 & -i & 0 \\ 0 & 0 & 0 & 0 & 0 & i & 0 & 0 \\ 0 & 0 & 0 & 0 & -i & 0 & 0 & 0 \\ 0 & 0 & 0 & i & 0 & 0 & 0 & 0 \\ 0 & 0 & 0 & 0 & 0 & 0 & 0 & 0 \end{pmatrix},$$

which is found by interpreting the commutation relation $[\lambda^{1,\text{adjoint}}, \lambda^A] = 2if_{1AB}\lambda^B$ as the action of $\lambda^{1,\text{adjoint}}$ on λ^A , where each λ^A is assigned to a trivial column vector with a 1 and the A^{th} index and zeroes everywhere else.

1.3.2 Properties of QCD

Quantum chromodynamics is a rich and complicated theory, which gives rise to many interesting phenomena.

1.3.2.1 Confinement

The first property of QCD to be discussed is **confinement**, which is simply the observation that quarks and gluons are never seen in isolation. Instead, they are *confined* inside of the color neutral bound states known as hadrons. This property is mostly understood in terms of the coupling constant g_s . The renormalization **QCDRenorm** of QCD gives rise to a g_s that varies with energy scale or distance. As the distance between two quarks increases, so too does g_s . At some point, the coupling becomes so strong that the energy required to separate the quarks is enough to create a quark-antiquark pair from the vacuum. Thus any attempts to pluck a quark from a hadron will always result in the creation of a new hadron, making it impossible to observe single quarks in isolation.

The large coupling constant makes it impossible to describe this phenomenon using perturbative techniques, so the exact mechanism of confinement is still not fully understood. However, it is often described using the phenomenological Lund string model **LundString**. In this model, the field lines of two quarks are pulled

together due to the self-interaction of the gluons. This creates a string-like structure between the two quarks, with a potential given by

$$V(r) \approx -\frac{4}{3} \frac{\alpha_s}{r} + \kappa r, \quad (1.5)$$

where r is the distance between the two quarks, $\alpha_s = \frac{g_s^2}{4\pi}$ and κ is the string tension. This is in contrast to the potential between two electrically charged particles, where the field lines are not pulled together and become less dense as the distance between the two particles increases. A schematic of these differences can be seen in Figure 1.4.

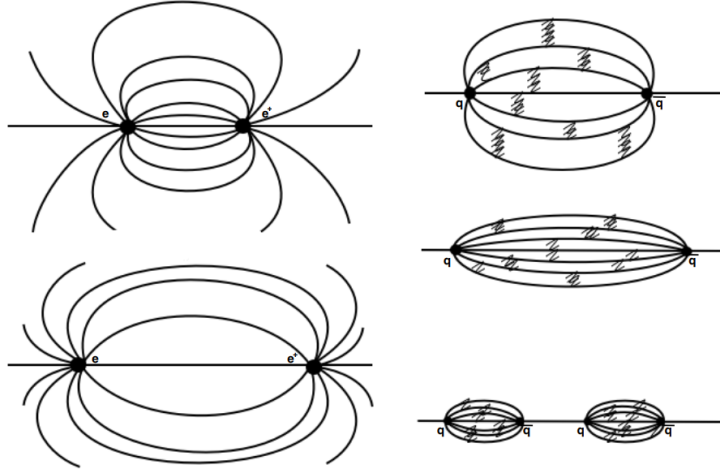


Figure 1.4: A schematic of the field lines between two electrically charged particles (left) and two quarks (right). The field lines between the quarks are pulled together due to the self-interaction of the gluons, whereas the electric field lines are not.

1.3.2.2 Asymptotic freedom

Just as the coupling constant becomes large at low energies and large distances, it also becomes small at high energies and small distances. This property is known as **asymptotic freedom**: at high enough energies, the quarks and gluons can be thought of as “free”, and their interactions can be modeled using perturbative QCD (pQCD). As discussed in Section ??, the discovery of asymptotic freedom in QCD was what allowed for the accurate predictions of the results of high energy particle collision experiments like SLAC [37]. The results of such experiments have also been used to calculate the value of the coupling constant itself at different energy

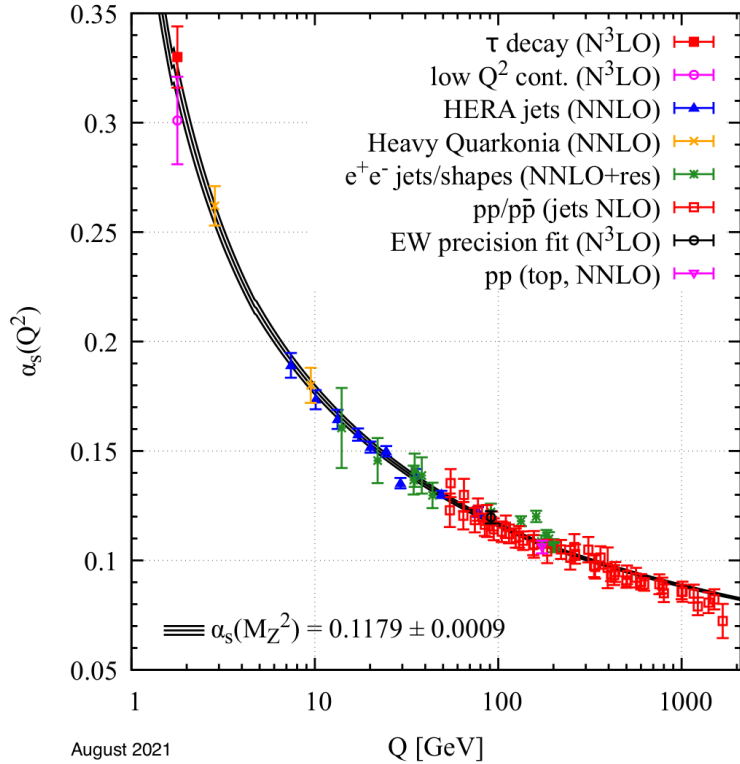


Figure 1.5: The value of the strong coupling constant α_s as a function of momentum transfer Q , which represents the energy scale of the interaction.

scales, as shown in Figure 1.5. The value of α_s at the Z^0 mass is also given in the figure, which is the most accurate measurement of α_s to date **PDG**.

1.3.2.3 Jets

During high energy particle collisions (between two protons, for example), the constituent partons of the protons will sometimes scatter off each other in a way that converts most of their initial longitudinal momentum (along the collision axis) into transverse momentum. Such a scattering is often referred to as a **hard scattering**. Because the momentum transfer is large, the cross section of the parton-parton scattering is calculable using pQCD. Furthermore, branching processes of the high momentum partons—like gluon radiation—can also be calculated perturbatively. Eventually, however, the partons will lose enough energy such that their behavior can no longer be described using perturbative techniques.

Luckily, the aforementioned Lund model is well equipped to deal with lower energy partons. Under the Lund model, as these colored partons move away from each other, the force between them increases until there is enough energy to produce a quark-antiquark pair (as discussed in Section 1.3.2.1). This process—known as string fragmentation—continues until the partons are no longer energetic enough to move away from each other, at which point they hadronize into a large number of color neutral bound states. These hadrons are roughly collimated in the direction(s) of the initial hard scattering, forming sprays of particles that may end up being seen by a detector. These hadronic showers are known as **jets**. and they are one of the first experimentally observed predictions of QCD. A diagram depicting the formation of a jet from an initial hard scattering of partons can be seen in Figure 1.6.

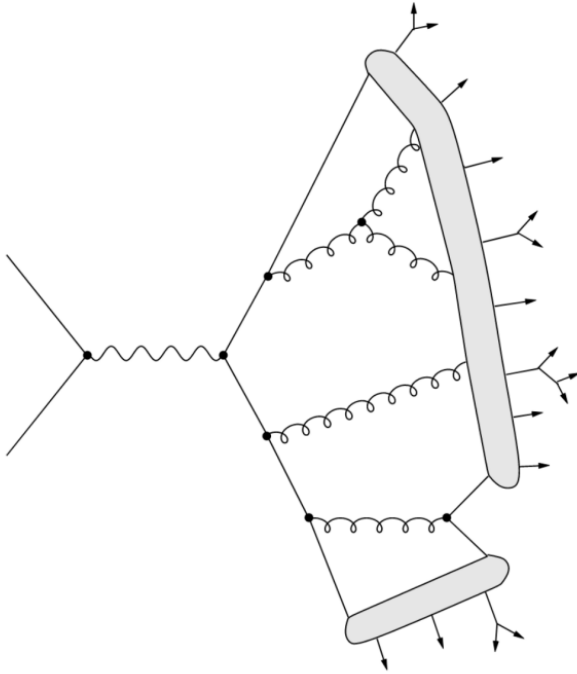


Figure 1.6: A diagram depicting the formation of a jet within the Lund model from an initial hard scattering of partons, adapted from [41]. The vertices represent perturbative QCD processes, the shaded regions represent string fragmentation/hadronization, and the outgoing arrows represent the resulting hadrons (which may decay further).

Jets serve as a useful experimental probe to study the strong interaction: they combine the perturbative and non-perturbative regimes of QCD, and they are rela-

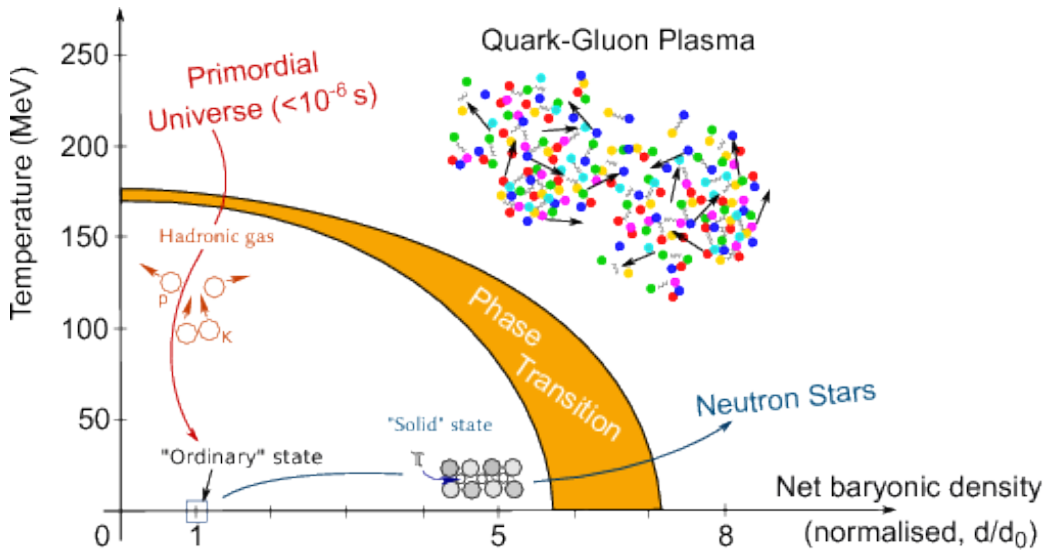


Figure 1.7: A phase diagram of the QGP, taken from [QGPPhaseDiagram](#). The axes are temperature and baryon density, and the orange band represents the phase transition from normal hadronic matter to the QGP.

tively easy to identify in a detector.

1.3.3 The Quark-Gluon Plasma

One of the most exciting consequences of the asymptotic freedom of QCD is the existence of a new state of matter at extreme temperatures and densities: the **quark-gluon plasma** (QGP) [QGP1](#), [QGP2](#). In this plasma, the quarks and gluons are not confined inside hadrons, and instead behave as quasi-free particles. This is analogous to an electromagnetic plasma, where electrons and protons are dissociated from their atoms. A phase diagram of this plasma can be seen in Figure 1.7. This diagram has two axes: temperature and baryon density. Increasing *either* of these quantities beyond a certain threshold will cause a phase transition from normal hadronic matter to the QGP. Similarities can be drawn between this phase diagram and that of a snowball: both heating *and* squeezing a snowball will cause it to melt into a liquid¹⁸.

Studying the QGP and its formation is interesting for a number of reasons, but those reasons often get lost in the cosmological hype: the universe is thought to have

¹⁸Be careful: if you continue to heat up the snowball enough, or squeeze hard enough, it will undergo another phase transition into the QGP.

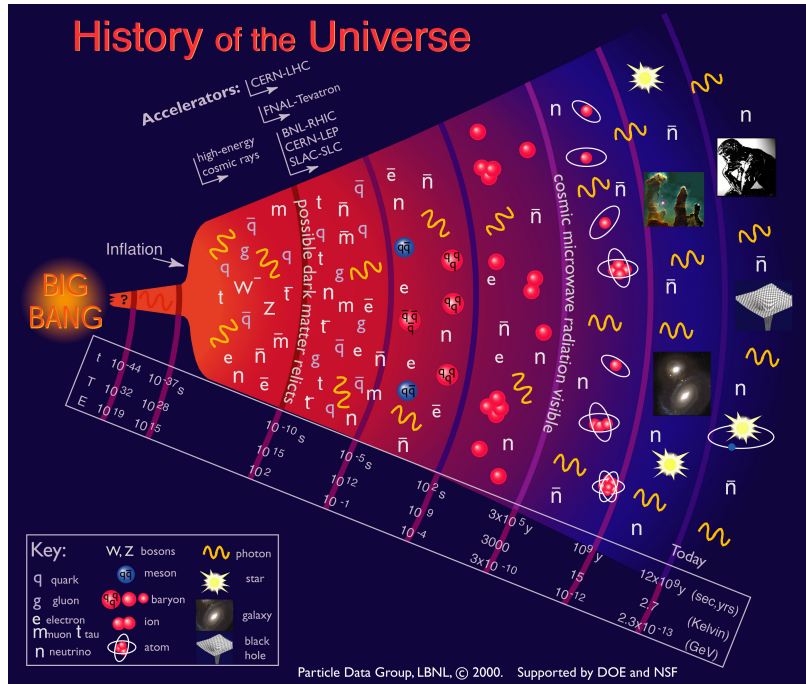


Figure 1.8: A schematic of the evolution of the universe, taken from **QGPUniverse**. The QGP phase of the universe on this diagram lies roughly between 10^{-10} and 10^{-5} seconds after the Big Bang.

been composed of this plasma in the first few microseconds after the Big Bang **QGP3**. Thus studying the QGP *can* give insight to the early universe and its expansion, which is schematically represented in Figure 1.8. It is also postulated that QGP formation occurs in the cores of neutron stars **QGPNeutron**, giving another avenue of interest for astrophysicists.

However, the QGP is also very interesting from a purely particle physics perspective: it is a highly non-perturbative QCD system that can be generated in a laboratory setting. Studying this plasma and its properties can help illuminate the dark, confounding corners of QCD that are not yet understood—like confinement. Unfortunately producing this plasma in a laboratory setting is not a trivial task, and requires¹⁹ colliding heavy ions at very high energies.

¹⁹There are hints of QGP formation in proton-proton collisions, which will be discussed in Section ??

1.4 Heavy ion collisions

The QGP phase diagram in Figure 1.7 shows two methods for producing the QGP: increasing the system's temperature or increasing its baryon density. Luckily these two methods are not mutually exclusive:

- Baryon density can be increased by looking at systems with a lot of baryons packed together (like the nucleus of a lead atom)
- Temperature can be increased by smashing the aforementioned systems together at higher energies (like in a particle accelerator)

Thus one of the best (and only) ways to study the QGP in a laboratory setting is through relativistic **heavy ion collisions**: the smashing together of two heavy nuclei at very high energies using a particle accelerator.

Unfortunately producing the QGP in this manner has a major drawback: while it is possible to heat up the system beyond the critical temperature required for QGP formation, the system expands and cools *very* quickly. For example, the QGP produced by colliding lead ions with center-of-mass energy $\sqrt{s_{NN}} = 2.76 \text{ TeV}$ at the Large Hadron Collider (LHC) only lasts for around $3 \text{ fm}/c$ **QGPFormation**, or 10^{-23} seconds. A diagram depicting the formation and evolution of the QGP in a heavy ion collision can be seen in Figure 1.9. This diagram can be split up into the following stages:

1. The Lorentz-contracted nuclei approach each other at very high energies, and the partons within the nuclei scatter off each other. ($t = 0 \text{ fm}/c$)
2. As new partons are created from the initial scatterings, the energy density of the system increases. Eventually this energy density is high enough to create the QGP. ($t \approx 1 \text{ fm}/c$)
3. Once the QGP is formed, it expands and cools in a hydrodynamic manner.
4. After the QGP cools below the critical temperature, the partons begin to hadronize, resulting in the formation of a hadron gas. ($t \approx 3 \text{ fm}/c$)
5. The hadron gas will continue to expand until the hadrons within the gas are no longer strongly interacting with each other. ($t \approx 10 \text{ fm}/c$) This is often broken up into two stages:

- The hadrons cease to interact *inelastically*, called **chemical freeze-out**.
 - The hadrons cease to interact *elastically*, called **kinetic freeze-out**.
6. If a detector is built within a few meters around the collision point, the final state hadrons can be observed. ($t \approx 10^{15} \text{ fm}/c$)

The last stage of this diagram is perhaps the most frustrating: it is only possible to study the QGP by observing the final state hadrons. Luckily there are some key observables associated with those final state hadrons that can shed light on the formation and evolution of this exciting plasma. Before those observables can be discussed, however, it is necessary to introduce a key concept in heavy ion collisions: the centrality of the collision.

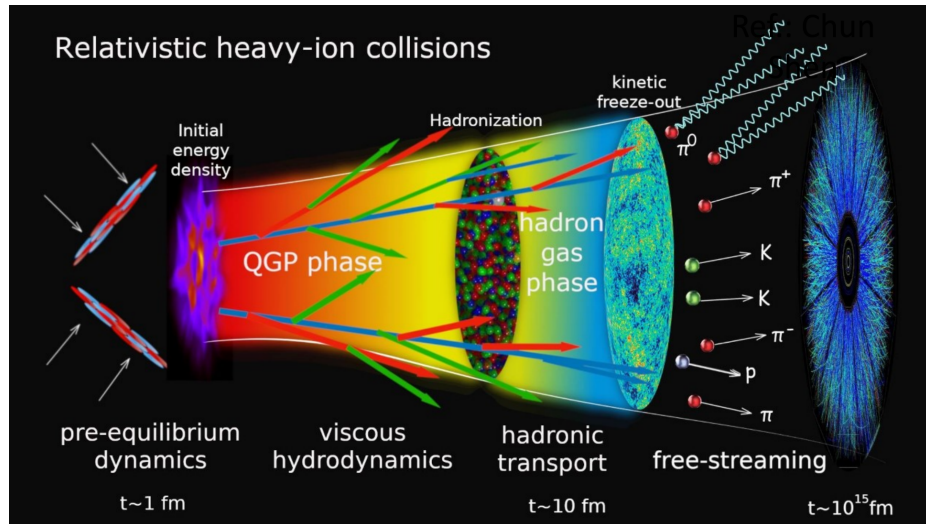


Figure 1.9: A schematic of the formation and evolution of the QGP in a heavy ion collision. The QGP is formed in the overlap region of the two colliding nuclei, and then expands and cools very quickly.

1.4.1 Collision centrality

The very first step of the heavy ion collision process involves the scattering of the partons within the two nuclei. However, these nuclei are not point-like objects: they have a finite size, and therefore need not collide “head-on”. Instead, the nuclei can collide at different **impact parameters** (commonly denoted as b), as shown in

Figure 1.10. The impact parameter is defined as the distance between the centers of the two nuclei, measured in the transverse plane (the plane perpendicular to the initial directions of the nuclei). Collisions with a large impact parameter give rise to *spectator* nucleons, which do not participate in the collision and continue traveling as they please.

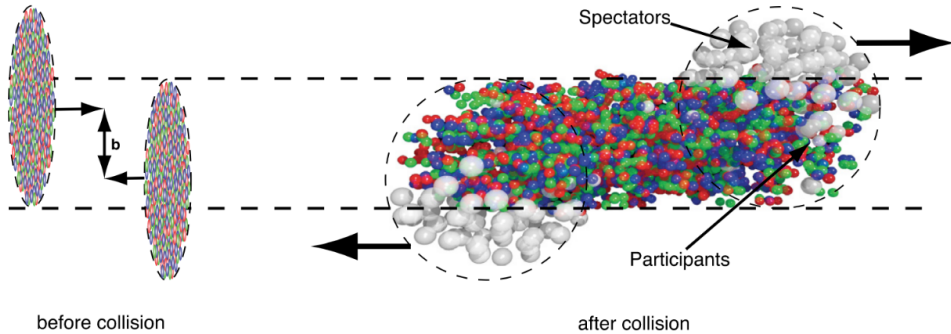


Figure 1.10: A schematic of a heavy ion collision with impact parameter b , taken from ??.

The impact parameter is very important when studying the QGP for a fairly straightforward reason: as the impact parameter decreases, the number of partonic scatterings increases, which in turn increases the energy density of the system. In some sense, the size of the impact parameter determines whether or not the QGP is formed in the subsequent stages of the collision. As such, characterizing heavy ion collisions by their impact parameter is quite useful. Unfortunately, much like the QGP, the impact parameter is not directly measurable and must be inferred from the final state hadrons.

Instead of classifying collisions based off their unobtainable impact parameter, they are instead classified by their **collision centrality**. The collision centrality is defined as

$$c = \frac{\int_0^b d\sigma/db'db'}{\int_0^\infty d\sigma/db'db'} = \frac{1}{\sigma_{AA}} \int_0^b \frac{d\sigma}{db'} db', \quad (1.6)$$

where σ_{AA} is the total cross section of the nucleus-nucleus (A-A) collision. As this number is strictly between 0 and 1, it is often expressed as a percentile: 0% corresponds to the most central collisions (lowest impact parameters), and 100% corresponds to the most peripheral collisions (highest impact parameters). If a monotonic

relationship between b and the number of final state particles seen in the detector is assumed, the collision centrality can be experimentally determined **MonotonicMultiplicity**. The number of final state particles from a collision is called the **multiplicity** of the collision, and is often denoted as N_{ch} . The subscript ch indicates that only charged particles are counted, as neutral particles are not seen by most detectors.

In practice, the collision centrality percentiles are usually determined by looking at the distribution of events as a function of the signal (effectively N_{ch}) as measured by a particular detector. The percentile for a specific event can then be determined by integration:

$$c \approx \frac{1}{\sigma_{AA}} \int_{N_{\text{ch}}}^{\infty} \frac{d\sigma}{dN'_{\text{ch}}} dN'_{\text{ch}}, \quad (1.7)$$

where N_{ch} is the multiplicity of the event in question. An example of separating events into centrality percentiles using this method can be seen in Figure 1.11. In this plot, Pb–Pb collisions are characterized by their event activity in the ALICE VZERO detector (which will be discussed in more detail in the next chapter). The red points correspond to fits obtained using Monte Carlo simulations based off of the Glauber model **GlauberModelALICE1**, **GlauberModelALICE2**. The Glauber model **GlauberModel** is a geometric model that treats the nuclei as a collection of nucleons, and models the collisions as a superposition of binary nucleon-nucleon collisions. This model gives a relationship between the impact parameter b , the number of participating nucleons N_{part} , and the number of binary nucleon-nucleon collisions N_{coll} . While not of particular import to this thesis, fitting the Glauber model to the data actually allows for the determination of the impact parameter corresponding to a given multiplicity percentile. The fact that the model describes the data well also serves as a sanity check for the experimental estimation of the collision centrality. In this thesis, the terms “multiplicity percentile” and “collision centrality” will be used interchangeably.

The approximation given by Equation 1.7 has an additional benefit: it allows for the determination of centrality without a clearly defined impact parameter. This is useful for proton-proton and proton-lead collisions, where the impact parameter is ill defined.

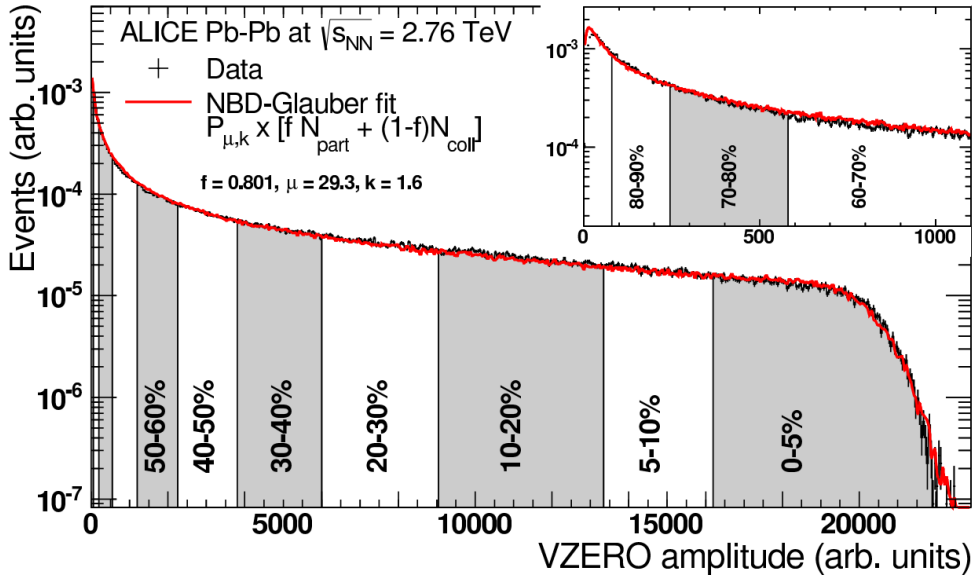


Figure 1.11: The distribution of Pb–Pb collision events as a function of event activity in the ALICE VZERO detector, taken from **ALICE**Centrality.

1.5 Theoretical models

Theoretical models of heavy ion collisions are pertinent to the understanding of QCD and the QGP. Without them, there would be no framework for interpreting the results from the very expensive experiments dedicated to studying this strongly interacting plasma. Unfortunately due to the complexity of these heavy ion collision systems, there is no *single* model that can describe the entire collision evolution. Instead, the choice of model to compare a particular observable to depends very heavily on the observable in question. For example, some models treat the QGP phase of the collision as a hydrodynamic system, washing out information about the initial partonic scatterings **EPOS**. This can be useful when trying to study bulk properties of the QGP (like the v_2 from Section ??), but not-so-useful when studying jets and their constituents. Other models focus more on the individual partonic scatterings and subsequent hadronization, but do not include an explicit QGP phase **Pythia**, **DPMJet**. Such models are powerful tools for analyzing smaller collision systems (pp and lower multiplicity p–Pb), but fail to capture many of the features observed in heavy ion collision data. In this section, the models used to help interpret the results of this

thesis will be discussed. All of these models are capable of simulating pp, p–Pb and Pb–Pb events.

1.5.1 PHSD

Parton-Hadron-String-Dynamics (PHSD) **PHSD1**, **PHSD2** is the only model explored in this thesis that utilizes a **microscopic transport approach**: it simulates the full space-time evolution of a heavy-ion collision by modeling the interactions of individual particles. Here “particles” refers to different quantities (strings, partons, hadrons) which are all evolved in different ways. The evolution of a collision within PHSD is as follows.

1.5.1.1 Initial stages

Prior to the collision, the simulation is broken up into a 3D-grid of size 56 in each of the x, y and z directions. The total size of the grid increases with each time step such the number of particles within a given cell evolves smoothly with time. The initial momentum distribution and abundances of partons within the nuclei (prior to any collision) are given by the thermal distributions

$$f(\omega, \vec{p}) = C_i p^2 \omega \rho_i(\omega, \vec{p}) n_{F/B}(\omega/\tau), \quad (1.8)$$

where ρ_i are the spectral functions of the quarks and gluons ($i = q, \bar{q}, g$) and $n_{F/B}$ are the Fermi-Dirac (for quarks) and Bose-Einstein (for gluons) distributions. Once the nuclei collide, the partons interact with each other under the Lund string model to form *leading hadrons* and *pre-hadrons*, as shown in Figure ???. The leading hadrons are immune to dissociation within the QGP, while the pre-hadrons are not.

1.5.1.2 QGP phase

If the energy density ϵ of a given cell increases beyond the critical energy density $\epsilon_c = 0.5 \text{ GeV/fm}^3$, the pre-hadrons within that cell are dissolved into partons. The partons are then treated as interacting quasi-particles under the DQPM **DQPM** model, with Lorentzian spectral functions given by

$$\cdot \quad (1.9)$$

where i is one of (q, \bar{q}, g) and the width γ_i is given by

$$(1.10)$$

The parameters X, Y, Z are fit to lattice QCD (lQCD) results at zero baryon chemical potential ($\mu_B = 0$).

1.5.2 EPOS LHC

In the EPOS LHC **EPOS LHC** model, the initial colliding nuclei results in many parton-parton scatterings happening in parallel, as shown in Figure 1.12. These simultaneous scatterings form a parton ladder, which are modeled as relativistic Lund strings. Long before hadronization, the model separates into two distinct parts: the *core* and the *corona*. This designation is based on the string density, i.e. the number of string segments per unit volume. If the string density exceeds a critical density ρ_c , the string segments are considered to be in the core. Otherwise, they are in the corona.

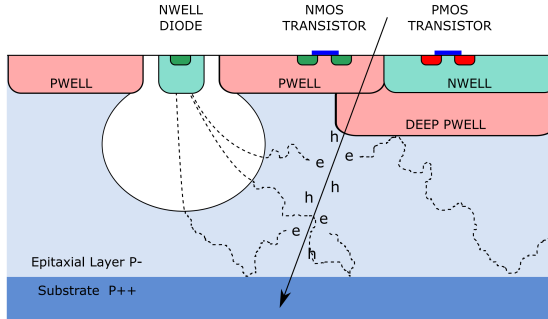


Figure 1.12: A schematic of the parton ladder in the EPOS LHC model.

The core is evolved in a hydrodynamic manner, which loses all information about the initial string segments and their interactions. Hadronization in the core is handled by a microcanonical procedure known as Cooper-Frye freeze-out, which is described in detail in **CooperFrye**. The core is associated with the QGP medium, and dominates particle production at higher multiplicities. The corona, however, corresponds to unmodified Lund string fragmentation, which dominates at large rapidity and in lower multiplicity events.

1.5.3 DPMJET

Perhaps the most simple²⁰ event generator explored in this thesis is the DPMJET [42] model. DPMJET combines the Dual Parton Model (DPM) **DPM** with the Lund string model **LundString** to describe proton-proton, proton-nucleus and nucleus-nucleus collisions across a large range of energies. The DPM describes all of the soft, non-perturbative multi-particle events that occur within a heavy ion collision using various large N_c and N_f limits of QCD. This is the only model explored in this thesis that does not have an explicit QGP phase, as the collision constituents²¹ are always treated independently. Thus DPMJET serves as a good baseline for vacuum fragmentation, and can be compared with other models (and data) to help quantify the effects of the explicit QGP phase.

²⁰Still *extremely* complicated, but has the least moving parts.

²¹Strings. It's always strings.

Bibliography

- [1] B. Pullman, *The Atom in the History of Human Thought*. Oxford: Oxford University Press, 1998, ISBN: 978-0-19-515040-7 (cit. on p. 2).
- [2] J. Dalton, “Experimental enquiry into the proportion of the several gases or elastic fluids, constituting the atmosphere,” *Memoirs of the Literary and Philosophical Society of Manchester*, vol. 1, pp. 244–258, 1805 (cit. on p. 2).
- [3] E. R. Scerri, *The Periodic Table: A Very Short Introduction*. Oxford University Press, Jul. 2019, pp. 117–123, ISBN: 9780198842323. DOI: 10.1093/actrade/9780198842323.001.0001. [Online]. Available: <https://doi.org/10.1093/actrade/9780198842323.001.0001> (cit. on p. 2).
- [4] D. Mendeleev, “The natural system of elements and its application to the indication of the properties of undiscovered elements,” *Journal of the Russian Chemical Society*, vol. 3, pp. 25–56, 1871 (cit. on p. 2).
- [5] I. Falconer, “J J Thomson and the discovery of the electron,” *Physics Education*, vol. 32, no. 4, p. 226, 1997. DOI: 10.1088/0031-9120/32/4/015. [Online]. Available: <https://dx.doi.org/10.1088/0031-9120/32/4/015> (cit. on p. 3).
- [6] E. Rutherford, “The scattering of α and β particles by matter and the structure of the atom,” *Philosophical Magazine Series 6*, vol. 21, pp. 669–688, 1911 (cit. on p. 3).
- [7] J. Chadwick, “Possible existence of a neutron,” *Nature*, vol. 129, p. 312, 1932 (cit. on p. 3).
- [8] C. D. Anderson, “The apparent existence of easily deflectable positives,” *Science*, vol. 76, no. 1967, pp. 238–239, 1932. DOI: 10.1126/science.76.1967.238. eprint: <https://www.science.org/doi/pdf/10.1126/science.76.1967.238>. [Online]. Available: <https://www.science.org/doi/abs/10.1126/science.76.1967.238> (cit. on p. 3).

- [9] S. H. Neddermeyer and C. D. Anderson, “Note on the nature of cosmic-ray particles,” *Phys. Rev.*, vol. 51, pp. 884–886, 10 1937. DOI: 10.1103/PhysRev.51.884. [Online]. Available: <https://link.aps.org/doi/10.1103/PhysRev.51.884> (cit. on p. 3).
- [10] R. Brown *et al.*, “Observations with Electron-Sensitive Plates Exposed to Cosmic Radiation,” *Nature*, vol. 163, no. 4133, pp. 82–87, Jan. 1949. DOI: 10.1038/163082a0 (cit. on p. 3).
- [11] V. D. Hopper and S. Biswas, “Evidence concerning the existence of the new unstable elementary neutral particle,” *Phys. Rev.*, vol. 80, pp. 1099–1100, 6 1950. DOI: 10.1103/PhysRev.80.1099. [Online]. Available: <https://link.aps.org/doi/10.1103/PhysRev.80.1099> (cit. on p. 3).
- [12] A. Barbaro-Galtieri *et al.*, “Apparent violation of the $\Delta S = \Delta Q$ rule by leptonic Σ^+ decay,” *Phys. Rev. Lett.*, vol. 9, pp. 26–29, 1 1962. DOI: 10.1103/PhysRevLett.9.26. [Online]. Available: <https://link.aps.org/doi/10.1103/PhysRevLett.9.26> (cit. on p. 3).
- [13] T. Nakano and K. Nishijima, “Charge Independence for V-particles,” *Progress of Theoretical Physics*, vol. 10, no. 5, pp. 581–582, 1953. DOI: 10.1143/PTP.10.581 (cit. on p. 3).
- [14] R. Serway, C. Moses, and C. Moyer, *Modern Physics*. Cengage Learning, 2004, pp. 12–13, ISBN: 9780534493394. [Online]. Available: <https://books.google.com/books?id=Yfo3rnt3bkEC> (cit. on p. 3).
- [15] M. Gell-Mann, “The Eightfold Way: A theory of strong interaction symmetry,” Mar. 1961. DOI: 10.2172/4008239. [Online]. Available: <https://www.osti.gov/biblio/4008239> (cit. on pp. 3, 4).
- [16] Y. Ne’eman, “Derivation of strong interactions from a gauge invariance,” *Nuclear Physics*, vol. 26, no. 2, pp. 222–229, 1961. DOI: 10.1016/0029-5582(61)90134-1 (cit. on p. 3).
- [17] W. Heisenberg, “Über den Bau der Atomkerne. I,” *Zeitschrift fur Physik*, vol. 77, no. 1-2, pp. 1–11, Jan. 1932. DOI: 10.1007/BF01342433 (cit. on p. 3).
- [18] M. Gell-Mann, “Isotopic Spin and New Unstable Particles,” *Physical Review*, vol. 92, no. 3, pp. 833–834, Nov. 1953. DOI: 10.1103/PhysRev.92.833 (cit. on p. 3).

- [19] T. Nakano and K. Nishijima, “Charge Independence for V-particles,” *Progress of Theoretical Physics*, vol. 10, no. 5, pp. 581–582, Nov. 1953. DOI: 10.1143/PTP.10.581 (cit. on p. 4).
- [20] M. Gell-Mann, “The interpretation of the new particles as displaced charge multiplets,” *Il Nuovo Cimento*, vol. 4, no. S2, pp. 848–866, Apr. 1956. DOI: 10.1007/BF02748000 (cit. on p. 4).
- [21] M. Gell-Mann, “A schematic model of baryons and mesons,” *Physics Letters*, vol. 8, no. 3, pp. 214–215, Feb. 1964. DOI: 10.1016/S0031-9163(64)92001-3 (cit. on p. 4).
- [22] A. Pickering, *Constructing quarks*. University of Chicago Press, 1999, pp. 114–125. DOI: 10.7208/chicago/9780226667997.003.0007 (cit. on p. 5).
- [23] B. J. Bjørken and S. L. Glashow, “Elementary particles and SU(4),” *Physics Letters*, vol. 11, no. 3, pp. 255–257, Aug. 1964. DOI: 10.1016/0031-9163(64)90433-0 (cit. on p. 5).
- [24] S. Glashow, “The hunting of the atoms and their nuclei: Protons and neutrons,” *New York Times*, Jul. 1976. [Online]. Available: <https://www.nytimes.com/1976/07/18/archives/the-hunting-of-the-atoms-and-their-nuclei-protons-and-neutrons.html> (cit. on p. 5).
- [25] S. L. Glashow, J. Iliopoulos, and L. Maiani, “Weak Interactions with Lepton-Hadron Symmetry,” *Phys Rev D*, vol. 2, no. 7, pp. 1285–1292, Oct. 1970. DOI: 10.1103/PhysRevD.2.1285 (cit. on p. 5).
- [26] H. Kendall, *Deep inelastic scattering: Experiments on the proton and the observation of scaling*, 1990. [Online]. Available: <https://www.nobelprize.org/uploads/2018/06/kendall-lecture.pdf> (visited on 08/21/2023) (cit. on pp. 5, 6).
- [27] J. Friedman, *Deep inelastic scattering: Comparisons with the quark model*, 1990. [Online]. Available: <https://www.nobelprize.org/uploads/2018/06/friedman-lecture.pdf> (visited on 08/21/2023) (cit. on p. 5).
- [28] R. Taylor, *Deep inelastic scattering: The early years*, 1990. [Online]. Available: <https://www.nobelprize.org/uploads/2018/06/taylor-lecture.pdf> (visited on 08/21/2023) (cit. on p. 5).

- [29] E. D. Bloom *et al.*, “High-Energy Inelastic e-p Scattering at 6° and 10° ,” *Physical Review Letters*, vol. 23, no. 16, pp. 930–934, Oct. 1969. DOI: 10.1103/PhysRevLett.23.930 (cit. on p. 5).
- [30] E. D. Bloom *et al.*, “High-Energy Inelastic e-p Scattering at 6° and 10° ,” *Physical Review Letters*, vol. 23, no. 16, pp. 930–934, Oct. 1969. DOI: 10.1103/PhysRevLett.23.930 (cit. on p. 5).
- [31] J. Bjorken, “Current algebra at small distances,” Jun. 2018. [Online]. Available: <https://www.osti.gov/biblio/1444446> (cit. on p. 6).
- [32] R. P. Feynman, “The behavior of hadron collisions at the uncertainties from these sources exhibit no multiplicity dependence, and a very small dependence on p_T . extreme energies,” in *Special Relativity and Quantum Theory: A Collection of Papers on the Poincaré Group*, M. E. Noz and Y. S. Kim, Eds. Dordrecht: Springer Netherlands, 1988, pp. 289–304, ISBN: 978-94-009-3051-3. DOI: 10.1007/978-94-009-3051-3_25. [Online]. Available: https://doi.org/10.1007/978-94-009-3051-3_25 (cit. on p. 6).
- [33] J. Aubert *et al.*, “Experimental observation of a heavy particle J ,” *Physical Review Letters*, vol. 33, Dec. 1974 (cit. on p. 6).
- [34] H. Fritzsch, M. Gell-Mann, and H. Leutwyler, “Advantages of the color octet gluon picture,” *Physics Letters B*, vol. 47, no. 4, pp. 365–368, Nov. 1973. DOI: 10.1016/0370-2693(73)90625-4 (cit. on p. 6).
- [35] D. J. Gross and F. Wilczek, “Ultraviolet Behavior of Non-Abelian Gauge Theories,” *Physical Review Letters*, vol. 30, no. 26, pp. 1343–1346, Jun. 1973. DOI: 10.1103/PhysRevLett.30.1343 (cit. on p. 7).
- [36] H. D. Politzer, “Reliable Perturbative Results for Strong Interactions?” *Physical Review Letters*, vol. 30, no. 26, pp. 1346–1349, Jun. 1973. DOI: 10.1103/PhysRevLett.30.1346 (cit. on p. 7).
- [37] P. Söding, *Twenty-five years of gluons*, 2004. [Online]. Available: <https://cerncourier.com/a/twenty-five-years-of-gluons/> (cit. on pp. 7, 14).
- [38] P. Söding, “On the discovery of the gluon,” *European Physical Journal H*, vol. 35, no. 1, pp. 3–28, Jul. 2010. DOI: 10.1140/epjh/e2010-00002-5 (cit. on p. 7).

- [39] A. Salam and J. C. Ward, “Weak and electromagnetic interactions,” *Il Nuovo Cimento*, vol. 11, no. 4, pp. 568–577, Feb. 1959. DOI: [10.1007/BF02726525](https://doi.org/10.1007/BF02726525) (cit. on p. 7).
- [40] S. Weinberg, “A Model of Leptons,” *Physical Review Letters*, vol. 19, no. 21, pp. 1264–1266, Nov. 1967. DOI: [10.1103/PhysRevLett.19.1264](https://doi.org/10.1103/PhysRevLett.19.1264) (cit. on p. 7).
- [41] R. K. Ellis, W. J. Stirling, and B. R. Webber, *QCD and Collider Physics* (Cambridge Monographs on Particle Physics, Nuclear Physics and Cosmology). Cambridge University Press, 1996. DOI: [10.1017/CBO9780511628788](https://doi.org/10.1017/CBO9780511628788) (cit. on p. 16).
- [42] S. Roesler, R. Engel, and J. Ranft, “The monte carlo event generator DPMJET-III,” in *Advanced Monte Carlo for Radiation Physics, Particle Transport Simulation and Applications*, Springer Berlin Heidelberg, 2001. arXiv: [0012252 \[hep-ph\]](https://arxiv.org/abs/0012252) (cit. on p. 26).